第 29 卷第 11 期 无 机 化 学 学 报 Vol.29 No.11
2013 年 11 月 CHINESE JOURNAL OF INORGANIC CHEMISTRY 2415-2421

层状、花形和棒状钛酸铋纳米结构的可控合成及光催化性能

林 雪*,[1] 于丽丽[1] 闫丽娜[1] 闫永胜[2] 关庆丰[3] 赵 晗[1]
([1]吉林师范大学化学学院,环境友好材料制备与应用教育部重点实验室,四平 136000)
([2]江苏大学化学化工学院,镇江 212013)
([3]江苏大学材料科学与工程学院,镇江 212013)

摘要:通过可控水热法,制备出层状、花形和棒状钛酸铋($Bi_4Ti_3O_{12}$,BIT)纳米结构。通过 X 射线衍射(XRD)和场发射扫描电子显微镜(FESEM)观测其结构和形貌特征。XRD 图显示,所制备的样品为层状钙钛矿结构。FESEM 结果表明,通过控制水热过程的反应参数可以得到不同形貌的纳米粉体。紫外–可见漫反射光谱(UV-Vis DRS)表明 BIT 样品的带隙能约为 2.63~2.95 eV。利用可见光(λ>420 nm)照射下的甲基橙降解实验评价了 BIT 样品的光催化性能。结果表明,BIT 的光催化活性比掺氮 TiO_2(N-TiO_2)高得多。所制备的层状 BIT 纳米结构光催化效率最高,经可见光照射 360 min,甲基橙溶液的降解率可达 95.0%。同时还研究了结构和形貌对不同条件下制备的 BIT 样品光催化活性的影响。

关键词:钛酸铋;层状;花形;棒状;可控合成;光催化降解
中图分类号:O643 **文献标识码**:A **文章编号**:1001-4861(2013)11-2415-07
DOI:10.3969/j.issn.1001-4861.2013.00.346

Controllable Synthesis and Photocatalytic Activity of Layered, Flowerlike, and Rodlike Bismuth Titanate Nanostructures

LIN Xue*,[1] YU Li-Li[1] YAN Li-Na[1] YAN Yong-Sheng[2] GUAN Qing-Feng[3] ZHAO Han[1]
([1]*College of Chemistry, Key Laboratory of Preparation and Application of Environmentally Friendly Materials of the Ministry of Education, Jilin Normal University, Siping, Jilin* 136000, *China*)
([2]*School of Chemistry and Chemical Engineering, Jiangsu University, Zhenjiang, Jiangsu* 212013, *China*)
([3]*School of Materials Science and Engineering, Jiangsu University, Zhenjiang, Jiangsu* 212013, *China*)

Abstract: Layered, flowerlike, and rodlike bismuth titanate ($Bi_4Ti_3O_{12}$, BIT) nanostructures were synthesized via the controllable hydrothermal method. The phase structures and morphologies were measured by X-ray diffraction (XRD) and field emission scanning electron microscopy (FESEM). XRD patterns demonstrate that the as-prepared samples are of layered-perovskite structure. FESEM shows that BIT crystals can be fabricated in different morphologies by simply manipulating the reaction parameters of hydrothermal process. The UV-Vis diffuse reflectance spectra (UV-Vis DRS) reveal that the band gaps of BIT photocatalysts are 2.63~2.95 eV. The as-prepared BIT photocatalysts exhibit higher photocatalytic activities in the degradation of methyl orange (MO) under visible light irradiation (λ >420 nm) compared with traditional N-doped TiO_2 (N-TiO_2). Layered BIT nanostructures show the highest photocatalytic activity. Up to 95.0% MO is decolorized after visible light irradiation for 360 min. In addition, the reason for the difference in the photocatalytic activities obtained at different conditions was studied based on the structures and morphologies.

Key words: bismuth titanate; layered; flowerlike; rodlike; controllable synthesis; photocatalytic degradation

收稿日期:2013-01-31。收修改稿日期:2013-05-28。
环境友好材料制备与应用教育部重点实验室项目和吉林省科技发展计划项目(20130522071JH)资助项目。
*通讯联系人。E-mail:jlsdlinxue@126.com

0 Introduction

Environmental pollution and the decreasing availability of fossil are two of the great challenges in the twenty-first century. Photocatalysis is expected to play an important role in helping to ease both environmental and energy issues by degrading toxic pollutants and splitting water for hydrogen production[1]. Semiconductors with large band gap, such as TiO_2 (3.2 eV) and ZnO (3.4 eV), have been widely used as photocatalysts[2-4]. However, the mismatch between the large band gap and the sunlight spectra limits the utilization of solar energy[5-6]. Therefore, many attempts have been made to prepare excellent visible-light-driven photocatalysts such as $ZnFe_2O_4$[7], Bi_2WO_6[8-9], Bi_2MoO_6[10], $BiVO_4$[11-12], $Bi_{12}TiO_{20}$[13], BiOBr[14], Bi_2LaTaO_7[15], and $Bi_4Ti_3O_{12}$(BIT)[16-17]. Among these visible-light catalysts, BIT has been found to show excellent visible-light-driven photocatalytic activity for water splitting and for the degradation of organic contaminants[16-18].

In $Bi_4Ti_3O_{12}$-based layered-perovskites, pseudo-perovskite blocks are interleaved with $(Bi_2O_2)^{2+}$ layers along the *c*-axis and an intra-electric field can be formed between them [19-20]. The bond angle of Ti-O-Ti is about 180°[21-22]. This special structure is beneficial in reducing the recombination of the charge carriers and is helpful for photocatalytic oxidation of organic pollutants, since it might stimulate the separation of electron-hole pairs and facilitate the mobility of photogenerated carriers to the surface of the crystals. It is, therefore, of interest to study the photocatalytic activity of BIT crystals. Photocatalytic properties of BIT have been examined. Kudo et al.[23] reported the preparation of BIT prepared by the solid-solid method and examined the photocatalytic activity of BIT for water splitting. Yao et al.[16] investigated the photocatalytic activity of BIT fabricated by using the chemical solution decomposition (CSD) method. Recently, we prepared BIT microspheres using a facile template-free hydrothermal approach[24]. In comparison with conventional nanoparticles prepared by a solid-state reaction, our prepared BIT exhibits an excellent visible-light photocatalytic performance because of its special microstructure, good permeability, and large surface area[22]. However, further research on the improvement of the BIT photocatalytic activity is still indispensable because of its poor quantum yield.

Since photocatalytic reaction occurs at the interface between reagent and photocatalyst, the control of both sizes and shapes of semiconductor photocatalyst has a profound influence on their photocatalytic activity[25]. Various methods have been utilized to prepare BIT, including solid-state reactions[23], chemical solution decomposition method[16], and hydrothermal processes[24]. In the preparation of photocatalysts, it is essential to control their crystallinity, sizes, structures, and morphologies, as these parameters are closely related to their photocatalytic activities. In addition, facile, cost-effective, and controllable synthetic routes associated with improved visible-light-photocatalysis should be developed considering the practical application of photocatalysts in the future. Among the various pathways, hydrothermal synthesis is a soft-chemical process widely used in preparing many kinds of functional materials[25]. The advantages of hydrothermal synthesis are that the experimental parameters such as the concentrations of reactants, the pH values, the temperature, and the reaction medium can be easily tuned to control the microstructures, and thus the properties and property dependent applications, of the target materials. On the basis of our previous work on the preparation of bismuth titanate[24], we have introduced a low-temperature solution-phase route to synthesize BIT particles with well controlled shapes. In this work, BIT photocatalysts with different morphologies have been prepared by means of a facile hydrothermal process, and methyl orange (MO) has been used as a model dye to evaluate the photocatalytic activity of the photocatalysts under visible light irradiation (λ >420 nm). The photocatalytic activities of the BIT catalysts with different morphologies have been discussed. The aim of the present paper is to study the influence of structure and morphology upon the optical properties and photocatalytic properties of BIT photocatalysts.

1 Experimental

1.1 Preparation of BIT photocatalysts

1.1.1 Synthesis of layered BIT sample

All the chemicals were analytically pure grade and used without further purification. Bismuth nitrate ($Bi(NO_3)_3 \cdot 5H_2O$) and tetrabutyl titanium ($Ti(OC_4H_9)_4$) were chosen as starting materials with the molar ratio of bismuth: titanium ions, 4:3. Polyvinyl alcohol (PVA) were used as surfactant. $Bi(NO_3)_3 \cdot 5H_2O$, $Ti(OC_4H_9)_4$, and PVA (0.125 mmol) were dissolved in 20 mL distilled water under vigorous stirring and then mixed with a potassium hydroxide solution. Before being transferred to a 20 mL stainless steel autoclave, the solution mixture was prepared under an ultrasonic water bath for 30 min in order to avoid the premature formation of bismuth titanate nuclei induced by the concentration of KOH and kept at a filling ratio of 70% (volume ratio). The autoclave was kept at 180 ℃ for 24 h and cooled to room temperature after the reaction. The precipitates were washed with deionized water and ethanol twice, separately. The final products were dried at 100 ℃ for 2 h in a vacuum box.

1.1.2 Synthesis of flowerlike BIT sample

The synthesis of flowerlike BIT sample was similar with that of layered BIT sample (as described in Section 1.1.1), except for the dosage of PVA (0.270 mmol).

1.1.3 Synthesis of rodlike BIT sample

Bismuth nitrate ($Bi(NO_3)_3 \cdot 5H_2O$) and tetrabutyl titanium ($TiCl_4$) were chosen as starting materials with the molar ratio of bismuth: titanium ions, 4:3. $Bi(NO_3)_3 \cdot 5H_2O$ and $TiCl_4$ were dissolved in 20 mL distilled water under vigorous stirring and then mixed with a potassium hydroxide solution (8 $mol \cdot L^{-1}$) and kept at a filling ratio of 70% (volume ratio). The autoclave was kept at 180 ℃ for 24 h and work-up of the products was described in Section 1.1.1.

1.2 Characterization of photocatalysts

The crystal structures of the samples were characterized by X-ray diffraction (XRD) on a Rigaku (Japan) D/max 2500 X-ray diffractometer (Cu $K\alpha$ radiation, λ=0.154 18 nm), employing a scanning rate of 4.00° $\cdot min^{-1}$, in the 2θ range from 20° to 50°. A field emission scanning electron microscopy (FESEM, Japan JEOL, JSM-6700F) was employed to observe the surface morphologies of the resulting samples. The surface areas of samples were measured by 3H-2000PS1 Surface Area & Pore size Analysis Instrument. Raman spectra of BIT samples were obtained by a micro laser Raman spectrometer (LabRam inva). Raman spectra were excited with the 514 nm line of an Ar^+ laser at an incident power of 20 mW. The optical properties were obtained by the photoluminescence (PL) measurement using HR800 LabRam Infinity Spectro photometer excited by a continuous He-Cd laser with a wavelength of 325 nm at a power of 50 mW. The UV-Vis diffuse reflectance spectra (DRS) were recorded for the dry-pressed disk sample using a scan UV-Vis spectrophotometer (UV-Vis, Japan SHIMADZU, UV-2550) equipped with an integrating sphere assembly.

1.3 Photocatalytic activities test

The photocatalytic degradation of methyl orange (MO) was employed to evaluate the photocatalytic activity of the samples. A 300 W Xe lamp (λ>420 nm) was used to provide visible light irradiation. A glass sheet was inserted between the lamp and the sample to filter out UV light (λ<420 nm). 0.10 g of photocatalyst was added to 100 mL of MO solution (0.01 $mmol \cdot L^{-1}$). Before irradiation, the suspensions were magnetically stirred in the dark for 30 min to ensure the adsorption-desorption equilibrium between the photocatalysts and MO. Then the solution was exposed to visible light irradiation under magnetic stirring. At given time intervals, 4 mL of suspension was sampled and centrifuged to remove the photocatalyst particles. Then, the catalyst-free dye solution was analyzed by a UV-2550 spectrometer to record intensity of the maximum band at 462 nm in the UV-Vis absorption spectra.

2 Results and discussion

Fig.1 shows XRD patterns of the as-prepared BIT products. All the reflection peaks can be indexed according to the PDF No.36-1486, suggesting that the

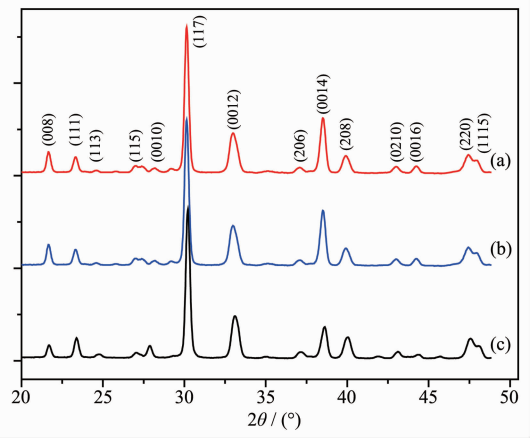

Fig.1 XRD patterns of BIT samples: (a) layered sample, (b) flowerlike sample, (c) rodlike sample

as-prepared products are of layered-perovskite structure ($Bi_4Ti_3O_{12}$). No peaks of impurities are detected from the patterns. The strong and sharp peaks indicate the high crystallinity of BIT samples.

The FESEM images of BIT samples prepared at different conditions are shown in Fig.2. It can be seen that in Fig.2(a) the crystals are plate shape. The nanoplates are parallel to each other forming layered products. One can see that in Fig.2(b) the nanoplates intersect with each other forming microflowers. It can be observed that in Fig.2(c) the crystals are rodlike, which have an average diameter of about 100 nm and a side length over 1 μm through their axial direction. In particular, no branching is observed for each nanorod, which implies that the nanorods are grown from a spontaneous nucleation and with high crystal perfection.

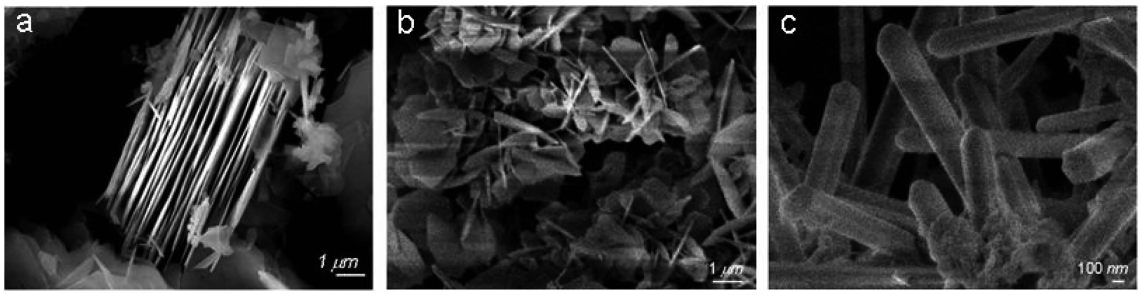

Fig.2 FESEM images of BIT samples: (a) layered sample, (b) flowerlike sample, (c) rodlike sample

It has been established that the photoluminescence (PL) spectra originate from the direct recombination of photoexcited electrons and holes[25]. In order to further study the efficient separation of photogenerated carriers in BIT, the corresponding photoluminescence (PL) spectra were obtained to disclose the migration, transfer and recombination process of photogenerated electron-hole pairs. Fig.3 shows the PL spectra of BIT samples measured at room temperature at an excitation wavelength of 325 nm. As shown, two PL bands near 439 nm and 500 nm are clearly observed in all the three kinds of BIT samples, which might arise respectively from the excitonic emission and surface-defect[25]. The fluorescence intensity of layered BIT sample is significantly weaker than that of flowerlike and rodlike products, which shows the recombination restraint of the e^-/h^+ pairs.

The UV-Vis DRS of the as-prepared BIT samples

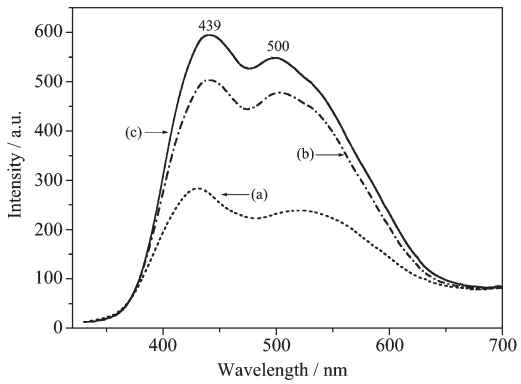

Fig.3 PL spectra of BIT samples: (a) layered sample, (b) flowerlike sample, (c) rodlike sample

are shown in Fig.4. As a comparison, the spectrum of N-TiO_2 was also measured. The absorption onset wavelength λ_g of layered, flowerlike and rodlike BIT samples are around 472 nm, 450 nm and 421 nm, respectively. The corresponding band gap energy E_g of BIT samples are 2.63, 2.76 and 2.95 eV, approximately, based on the formula: E_g=1 240/λ_g, showing

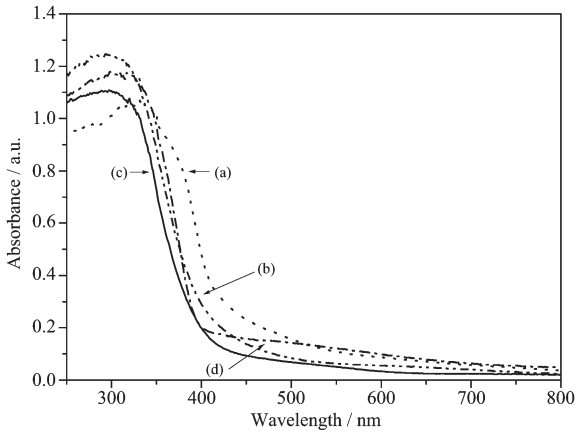

Fig.4　UV-Vis DRS of BIT samples: (a) layered sample, (b) flowerlike sample, (c) rodlike sample, (d) N-TiO_2

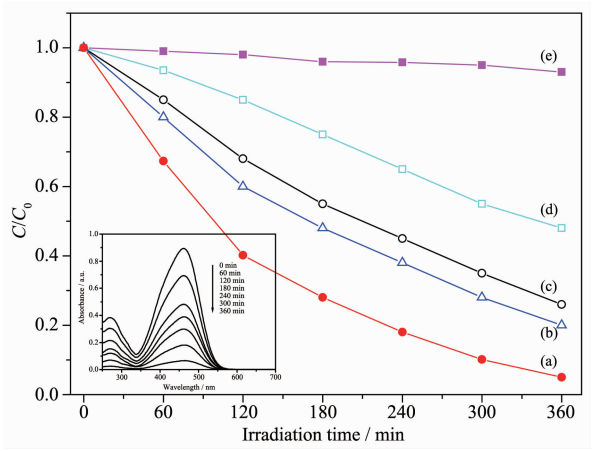

Fig.5　Temporal courses of the photodegradation of MO in different catalyst aqueous dispersions: (a) layered BIT sample, (b) flowerlike BIT sample, (c) rodlike BIT sample, (d) N-TiO_2, (e) without catalyst; Inset shows the UV-Vis spectral changes of MO by layered BIT sample

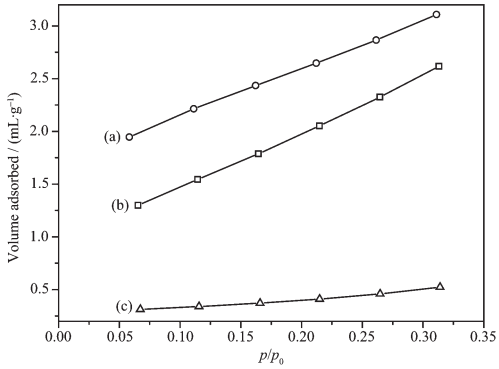

Fig.6　Nitrogen adsorption isotherms of (a) layered BIT sample, (b) flowerlike BIT sample, (c) rodlike BIT sample

marked red shift in the absorbance compared to N-TiO_2, due to the contribution of 6s electrons from Bi^{3+}[26]. It indicates that BIT photocatalysts have a suitable band gap for photocatalytic decomposition of organic contaminants under visible light irradiation. In addition, slight red shift of the absorption band edge of layered sample can be observed.

Photodegradation experiments of MO were carried out under visible light irradiation in order to test the photocatalytic performance of BIT photocatalysts. For comparison, the photodegradation of MO by N-TiO_2 and that without any catalyst were also carried out. From the catalytic studies, BIT samples are more photoactive towards MO solution than N-TiO_2 (Fig.5). Photocatalytic activities of BIT samples with different morphologies are shown in Fig.5. It shows that the degradation rate of MO by layerd sample increases to 95.0% after 360 min irradiation, much higher than that of flowerlike and rodlike sample.

According to the above analysis, layered BIT sample showing higher photocatalytic activity should have a larger surface area than that of flowerlike and rodlike sample. The nitrogen adsorption isotherms of BIT samples are presented in Fig.6. The measured BET specific surface areas of layered, flowerlike, and rodlike BIT are 10, 9, and 2 $m^2 \cdot g^{-1}$, respectively. Thus, the better performance of layered sample is related to its larger surface areas. Therefore, the different photodegradation rates of MO by different BIT samples indicate that the photocatalytic performances of these BIT samples are greatly different and strongly dependent on their morphologies.

Fig.7 displays the XRD patterns of layered BIT sample before and after 360 min of visible light irradiation. Both the position and the intensity of the peaks in the XRD pattern of layered BIT sample after irradiation are almost the same as those of layered BIT before irradiation. As shown, layered BIT is relatively stable to visible light under the present experimental conditions. This result indicates a possibility for the application of layered BIT sample

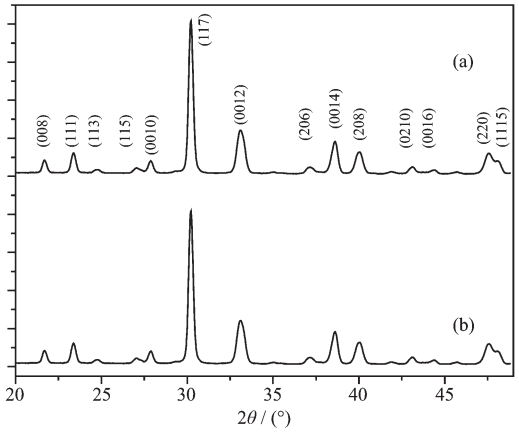

Fig.7 XRD patterns of layered BIT sample before a) and after b) photodegradation

in waste water treatment.

The stability tests results are shown in Fig.8. No significant decrease in catalytic activity is observed in the recycling reactions.

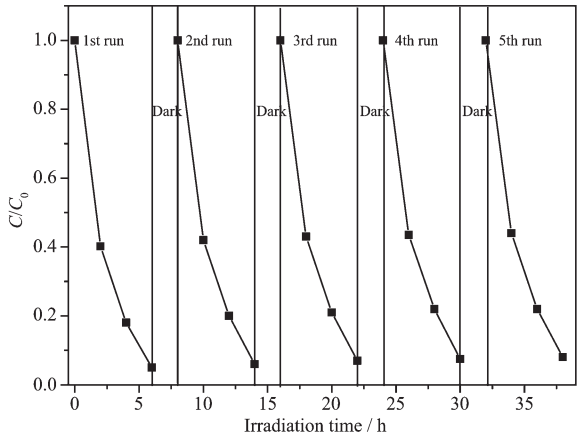

Fig.8 Stability evaluation for layered BIT sample: five reaction cycles for photodegradation of MO under visible light irradiation

Fig.9 shows FESEM image of layered BIT sample after recycling reactions. No significant change of the morphology of layered BIT sample is detected after recycling reactions. Combined with the XRD patterns, all evidences demonstrate that layered BIT sample has good stability.

The photocatalytic property of BIT is also related to the distortion of the M-O polyhedron in crystal structure. Raman spectra of BIT samples are shown in Fig.10. It can be observed that the as-prepared BIT samples exhibit modes only corresponding to $Bi_4Ti_3O_{12}$ orthorhombic structure, which is in agreement with

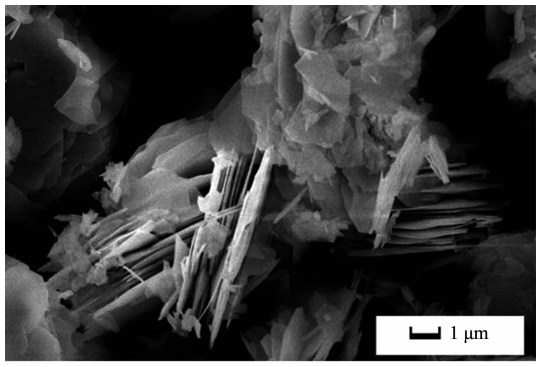

Fig.9 FESEM image of layered BIT sample after recycling reactions

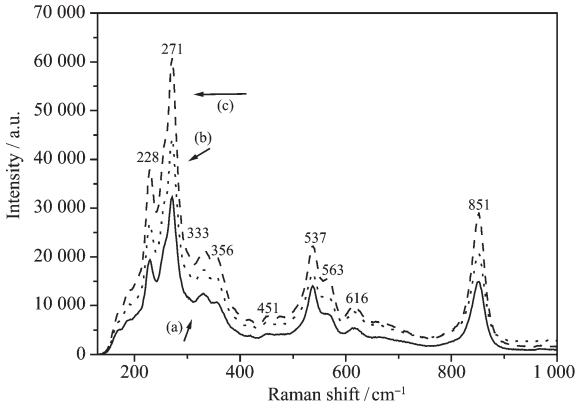

Fig.10 Raman spectra of BIT samples: (a) layered sample, (b) flowerlike sample, (c) rodlike sample

the literature [27]. The band at 271 cm^{-1} is ascribed to the Ti-O bending vibration modes into the TiO_6 octahedral, while the bands at 537 and 851 cm^{-1} correspond to the O-Ti-O stretching modes. However, an obvious change of the Raman band intensity occurs in this range. The dependence of the relative intensities of the bending vibration modes (271 cm^{-1}) of the TiO_6 octahedral on the synthesis conditions is observed, demonstrating that different space symmetries are formed and the variation or rearrangement of the crystal structure exists under the influence of reaction conditions. A similar Raman-band shift of the Mo-O stretching vibration is also observed in the Raman spectra of Bi_2MoO_6[28]. Several differences in half-widths and intensities of the diffraction peaks were observed in the XRD patterns of BIT samples synthesized hydrothermally at various conditions (Fig. 1), indicating that slight changes in the structure, even though all the powders exhibit the orthorhombic

structure. Based on the above results and analysis, it can be concluded that the changing of reaction parameters of hydrothermal process may influence the crystal structure and corresponding photocatalytic performance.

3 Conclusions

BIT photocatalysts with different morphologies have been synthesized through the controllable hydrothermal method. XRD results confirm that the composition of the as-fabricated samples is of layered perovskites. The energy band gaps of BIT samples are 2.63~2.95 eV. Due to the structure-property relationships, BIT photocatalysts exhibit enhanced visible photocatalytic activity over that of N-TiO_2 in the decomposition of MO in water. Our work suggests that the photocatalytic performance of BIT is greatly dependent on the local structure and the morphology.

References:

[1] Wang S L, Li P G, Zhu H W, et al. *Powder Technol.*, **2012**, **230**:48-53

[2] Tian G H, Jing L Q, Fu H G, et al. *J. Hazard. Mater.*, **2009**, **161**:1122-1130

[3] Chen F, Zou W W, Qu W W, et al. *Catal. Commun.*, **2009**, **10**:1510-1513

[4] LI Li(李丽), YANG He-Qing(杨合情), MA Jun-Hu(马军虎), et al. *Chinese J. Inorg. Chem.*(*Wuji Huaxue Xuebao*), **2012**, **28**(1):25-29

[5] YAN Ya(严亚), LÜ Ying(吕瑛), XIA Yi(夏怡), et al. *Chinese J. Inorg. Chem.*(*Wuji Huaxue Xuebao*), **2011**,**27**(10):1999-2004

[6] YU Chang-Lin(余长林), ZHOU Wan-Qin(周晚琴), YU Jimmy C. *Chinese J. Inorg. Chem.*(*Wuji Huaxue Xuebao*), **2011**,**27**(10):2033-2038

[7] Tahir Asif Ali, Upul Wijayantha K G. *J Photoch. Photobio. A*: *Chem.*, **2010**,**216**:119-125

[8] SONG Li-Hua(宋丽花), TAN Guo-Qiang(谈国强), XIA Ao (夏傲), et al. *Chinese J. Inorg. Chem.*(*Wuji Huaxue Xuebao*), **2011**,**27**(11):2133-2137

[9] Zhang L W, Wang Y J, Cheng H Y, et al. *Adv. Mater.*, **2009**,**21**:1286-1290

[10]Tian G H, Chen Y J, Meng X Y, et al. *ChemPlusChem*, **2013**,**78**:117-123

[11]Liu Y Y, Huang B B, Dai Y, et al. *Catal. Commun.*, **2009**, **11**:210-213

[12]Zhang Z J, Wang W Z, Shang M, et al. *Catal. Commun.*, **2010**,**11**:982-986

[13]Hou J G, Cao R, Jiao S Q, et al. *Appl. Catal. B*: *Environ.*, **2011**,**104**:399-406

[14]Zhang L, Cao X F, Chen X T, et al. *J. Colloid Interf. Sci.*, **2011**,**354**:630-636

[15]Luan J F, Hao X P, Zheng S R, et al. *J. Mater. Sci.*, **2006**, **41**:8001-8012

[16]Yao W F, Xu X H, Wang H, et al. *Appl. Catal. B*: *Environ.*, **2004**,**52**:109-116

[17]Yao W F, Wang H, Xu X H, et al. *Mater. Lett.*, **2003**,**57**: 1899-1902

[18]Wang Z Z, Qi Y J, Qi H Y, et al. *J. Mater. Sci.*: *Mater. Electron.*, **2010**,**21**:523-528

[19]Buscaglia M T, Sennour M, Buscaglia V, et al. *Cryst. Growth Des.*, **2011**,**11**:1394-1401

[20]Chen X H, J Q Hu, Chen Z W, et al. *Biosens. Bioelectron.*, **2009**,**24**:3448-3454

[21]Chen Z W, He X H. *J. Alloys Compd.*, **2010**,**497**:312-315

[22]Patwardhan J S, Rahaman M N. *J. Mater. Sci.*, **2004**,**39**:133-139

[23]Kudo A, Hijii S. *Chem. Lett.*, **1999**,**28**:1103-1104

[24]Lin X, Lü P, Guan Q F, et al. *Appl. Surf. Sci.*, **2012**,**258**: 7146-7153

[25]XU Di(许迪), GAO Ai-Mei(高爱梅), DENG Wen-Li(邓文礼), et al. *Acta Phys.-Chim. Sin.*(*Wuli Huaxue Xuebao*), **2008**,**24** (7):1219-1224

[26]Zhu X Q, Zhang J L, Chen F. *Chemosphere*, **2010**,**78**:1350-1355

[27]Oliveira R C, Cavalcante L S, Sczancoski J C, et al. *J. Alloys Compd.*, **2009**,**478**:661-670

[28]Zhang L W, Xu T G, Zhu Y F, et al. *Appl. Catal. B*: *Environ.*, **2010**,**98**:138-146